

LETTERS

Charge Separation Effects on the Rate of Nonradiative Relaxation Processes in Quantum Dots—Quantum Well Heteronanostructures

R. B. Little, C. Burda, S. Link, S. Logunov, and M. A. El-Sayed*

Laser Dynamics Laboratory, Georgia Institute of Technology, School of Chemistry and Biochemistry, Atlanta, Georgia 30332-0400

Received: May 18, 1998; In Final Form: June 30, 1998

Using time-resolved optical hole (oh)-burning techniques with femtosecond lasers, the time dependence of the spectral diffusion of the oh is examined for both the CdS quantum dot (QD) and the CdS/HgS/CdS quantum dot quantum well (QDQW) nanoparticles. It is found that the nonradiative relaxation of the optical hole is at least 3 orders of magnitude slower in the QDQW than in the QD system. Analysis of the second derivative of the broad transient bleach spectrum of the QDQW system in the 1.6–2.5 eV energy region at 50 fs delay time is found to have a minimum at 2.1 eV, corresponding to a minimum in the radiative probability. Around this energy, the rise and decay times of the transient bleach in the spectrum are found to change greatly. These results suggest that spectral diffusion in the QDQW is a result of relaxation from high- to low-energy exciton states, involving an intervening dark state at an energy of ~ 2.0 eV. The energies of the maxima and minimum of the second-derivative curve are found to be in good agreement with recent theoretical calculations by Jaskolski and Bryant¹ of the energies of the radiative and dark charge-separated state, respectively. In the latter, the hole is in the CdS clad and the electron is in the HgS well. The slow nonradiative relaxation processes involving this state are expected to be slow owing to the large change in the charge carrier effective masses as they cross from the CdS clad to the HgS well.

Introduction

The effects of quantum confinement and quantum size effects on the radiative processes of semiconductor nanoparticles (quantum dots, QD) as well as the electron–hole dynamics have been the subject of intensive study.^{2–21} These studies showed that as the particle size becomes smaller than the exciton Bohr radius, quantum confinement occurs, giving rise to an increase in the band gap energy and the absorption coefficient. The magnitude of band gap enlargement depends on the size of the nanoparticle (quantum size effect). The dimensionality of the exciton motion changes from 3-D to 0-D. Furthermore, the quality of the surface becomes important in determining the dynamics of the electron and hole trapping and recombination, thus producing the observed emission properties.^{22,23}

Nanoparticles have been synthesized and studied in which a core of CdS is covered with a shell of the much lower band gap material (HgS), which is then covered by another shell (clad) of CdS.²⁴ These quantum dot quantum well (QDQW) nanoparticles have shown luminescence resulting from electron and hole recombination in the lowest exciton level in the HgS QW.²⁵

Few studies have been carried out on the nonradiative relaxation of the high-energy exciton states in these nanoparticles. Using a subpicosecond laser, we have previously examined the relaxation of the optical holes (oh) in the CdS/HgS/CdS QDQW system created by excitation at 400 nm.²⁷ We observed a rather broad oh, which was first observed at slightly lower energy than the laser excitation energy, which diffused with time to even lower energy and which finally resided in

the QW lowest energy absorption region. Within the QW absorption region, the oh decayed with its normal decay time. We previously explained²⁷ these results by assuming the presence of different interfacial traps of lower energies than the excitation energy. The exact nature of these traps, i.e., if they are physical traps or intervening levels having relatively long nonradiative lifetimes, was not determined.

In the present study, using hole-burning techniques with a femtosecond laser, we attempted to burn an optical hole in CdS QD and compared its temporal behavior with that in the CdS/HgS/CdS QDQW. Contrary to the previous results for the QDQW system, we were *unable* to burn an oh in the CdS QD at high energy; neither were we able to observe spectral diffusion. With our time resolution, we can only observe the oh in the CdS QD system in the lowest exciton absorption band. These observations suggest that the spectral diffusion in the CdS QD system occurs much faster than our 100 fs pulse width and that the spectral diffusion in the QD (<100 fs) is much faster than that in the QDQW system (10 ps).

Recently, theoretical calculations^{1,26} have been carried out, giving the lower energy levels for exciton states in the CdS QD²⁶ and in the CdS/HgS/CdS QDQW.^{1,26} A number of conclusions can be reached from comparing the results of these calculations for the two systems. It is found that the introduction of the well has resulted in a red shift of the band gap energy of the nanoparticles as well as an increase in the energy separation between the different low-energy levels. In addition, it revealed the existence of optically forbidden transitions in the QDQW particles due to charge-separated states in which the electron and hole are trapped in different shells.¹ The question immediately arises as to the effect of these charge-separated states on the nonradiative relaxation processes. The transition probability of the nonradiative transitions between the charge-separated states and the lowest energy state (in which the electron and hole are in the well) is expected to be relatively small in heteronanostructured materials with large differences in their band gap energies owing to the fact that it involves the transport of one of the carriers from one shell to the other in which its effective mass is quite different.

In this communication, we present the results of the band shape analysis of the time-dependent optical transient bleach spectrum observed in the CdS/HgS/CdS QDQW system. From these spectra and the results on the rise and decay times of the bleach spectrum at different wavelengths, possible locations of the high-energy exciton states are identified and are found to be in reasonably good agreement with the calculated values.¹ The results strongly suggest the presence of a dark state at ~ 2.1 eV. This dark state is assigned as the $1S_{1/2} - 1S$ calculated dark state¹ in which *the hole is in CdS clad and the electron is in the HgS well*. The relaxation processes between this state and others, in which both carriers are in the same shell, are expected to have a small probability of nonradiative decay owing to the expected change in their effective mass.

Experimental Section

The CdS/HgS/CdS quantum dot quantum well was prepared in a manner similar to that described by Mews et al.²⁴ In general, the structure is fabricated by forming a CdS core, displacing the surface Cd^{2+} ions by Hg^{2+} ions, and reprecipitating the displaced Cd^{2+} ions around the deposited Hg^{2+} to form the CdS/HgS/CdS heteronanostructure. The CdS core was prepared from 500 mL of a 2×10^{-4} M $Cd(ClO_4)_2$ and 2×10^{-4} M sodium polyphosphate solution. The pH of the resulting solution was set to 9.4, and the solution was purged with argon

for 20 min. Afterwards 2.24 mL of H_2S was injected, and ripening occurred for 10 min. The resulting CdS colloid was purged for 40 min. Forty milliliters of 0.001 M $Hg(ClO_4)_2$ was then rapidly added to the CdS colloid, displacing surface Cd^{2+} ions and forming the CdS/HgS nanostructure. The CdS clad was deposited around the CdS/HgS structure by slowly titrating the colloid with 120 mL of 5×10^{-4} M H_2S solution. The added S^{2-} binds Cd^{2+} to form CdS, which deposits on the existing CdS/HgS to form the CdS/HgS/CdS QDQW. These techniques make CdS particles of 4–6 nm in diameter and QDQW particles of an average size of 6–7 nm. The absorption spectra were taken at the different steps of the preparation to compare with those of Mews et al.²⁴ to ensure that we are getting the same particles that were highly characterized in their work. The final QDQW particles obtained are found to have the same absorption (both in position and bandwidth) of the band gap transition as well as the higher energy exciton transition as those previously reported. Similarly, the emission and excitation spectra were also in good agreement.²⁴

Owing to the expected inhomogeneous nature of the colloidal particles in this system, hole-burning techniques, known to reduce the effect of the inhomogeneity on the observed spectrum, are used. Time-resolved hole-burning techniques were used in order to follow the rate of the spectral diffusion and thus the relaxation processes of the high-energy exciton states to the well (the band gap state).

The femtosecond hole-burning transient spectroscopy was carried out as follows: An amplified Ti-sapphire laser system (Clark MXR CPA 1000) was pumped by an argon ion laser (Coherent Innova 300). This produced laser pulses of 100 fs duration (HWHM) and an energy of 1 mJ at 790 nm. The repetition rate was 1 kHz. A small part (4%) of the fundamental was used to generate a white light continuum in a 1 mm sapphire plate. The remaining laser light was split into two equal parts in order to pump two identical OPAs (Quantronix TOPAS). Each produced signal and idler waves with a total energy of 150 μ J. Tunable excitation wavelengths in the visible range were then produced by SHG and SFG of the signal wave. The excitation beam was modulated by an optical chopper (HMS 221) with a frequency of 500 Hz. The second OPA was used to generate tunable probe wavelengths outside the continuum range. The probe light was split into a reference and a signal beam. After passing the monochromator (Acton Research), both beams were detected by two photodiodes (Thorlab). The kinetic traces were finally obtained using a sample-and-hold unit and a lock-in-amplifier (Stanford Research Systems). The typical measured optical density (OD) changes were in the range of 50 mOD. For spectral measurements a CCD camera (Princeton Instruments) attached to a spectrograph (Acton Research) was used. The group velocity dispersion of the white light continuum was compensated.

Results and Conclusions

Figure 1 compares the time dependence of the optical hole (bleached band) observed on the picosecond time scale for both the CdS QD (top) and the CdS/HgS/CdS QDQW nanoparticles. Excitation of both systems was carried out at 400 nm. It is obvious that no resonant oh is observed in either system at zero delay time, but usually the optical hole is observed at lower energies. While the band shape of the oh for the QDQW shows spectral diffusion as its shape and peak shift from high to low energy with time, the oh for the QD does not show such a large time-dependent spectral shift. The optical hole in the QD appears in the lowest energy absorption region immediately after

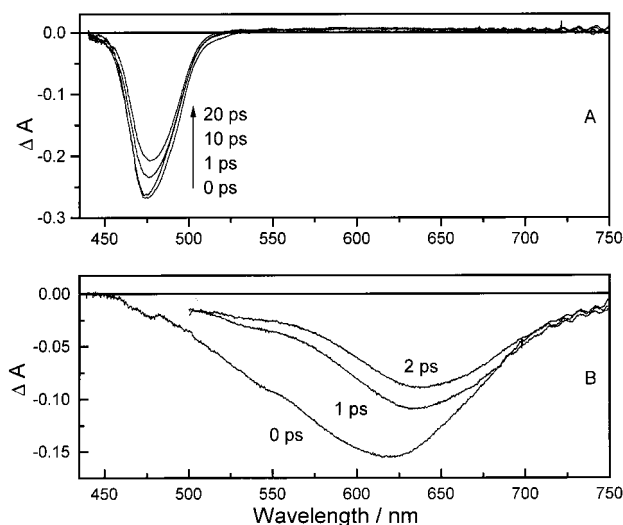


Figure 1. Time-resolved optical hole (bleach) spectra. The time dependence of the optical holes (oh) formed by pumping at 400 nm of the CdS quantum dot (top) and CdS/HgS/CdS quantum dot quantum well (QDQW) colloidal nanocrystals. Very rapid unresolved spectral diffusion from the pump wavelength region to the band gap absorption region is observed in the QD, but relatively slower time-resolved spectral diffusion is observed for the QDQW.

excitation and undergoes very slight red shift within 2.5 ps.²⁸ Previously, we have attributed the observed time dependence of the spectral diffusion of the optical hole in the QDQW to the presence of different interfacial traps.²⁷

Reexamining the oh spectra of the QDQW particles, using instruments with femtosecond time resolution and in light of the recent calculations of the exciton states^{1,26} for these nanoparticles, we began to consider the possibility that the observed temporal behavior of the optical hole of these particles is due to relaxation processes from higher to lower energy exciton levels. Owing to the reduction in the inhomogeneous broadening known to result from the hole-burning techniques, the 50 fs delay hole-burning spectrum (shown in broken line in Figure 2) was far better resolved than the absorption spectrum. The second derivative of the 50 fs delay spectrum is shown as an inset of Figure 2. This derivative spectrum shows clearly two maxima, one at 525 nm (2.36 eV) and the other at 625 nm (1.98 eV). Examining Figure 2, the maximum at 525 nm corresponds to a deconvoluted shoulder in the 50 fs bleach spectrum. The 625 nm maximum could result from overlapping absorptions of the first two allowed transitions predicted by Bryant et al.^{1,26} at 1.89 eV ($1P_{3/2} - 1P$) and 1.93 eV ($1P_{1/2} - 1P$). This assignment is supported by the observation that the maximum in the bleach spectrum shifts from 625 (1.98 eV) nm at 50 fs delay to 650 nm (1.91 eV) at 2.0 ps delay. It is interesting that the other maximum in the derivative spectrum at 2.36 eV could suggest the presence of another optically allowed absorbing state that has not as yet been calculated. The minimum between the two maxima could either suggest the presence of dark states, as predicted by the theoretical calculations,¹ or the absence of any exciton state. We studied the wavelength dependence of the exciton dynamics to distinguish between these two possibilities.

To probe the dynamics of the different excitonic states in more detail, we carried out kinetic studies by observing the formation and decay times of the optical hole (bleach) in the energy regions of these two optically allowed transitions, while pumping was carried out at 400 nm. The results are shown in Figure 3. It is clear that both the decay times and the formation times (inset) show different behaviors for the oh dynamics

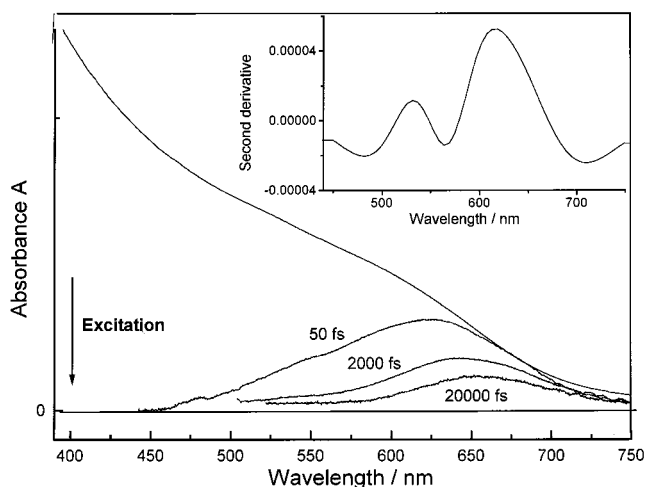


Figure 2. Comparison of the absorption spectra (top) and time dependence of the optical hole (bleach) spectra of the CdS/HgS/CdS quantum dot-quantum well colloidal nanocrystal. The inset gives the derivative of the bleach spectrum at 50 fs delay (top broken-line spectrum). The correspondence between these two peaks and the energy level structure theoretically calculated¹ suggested that spectral diffusion in this system results from relaxation involving the exciton levels of the QDQW nanoparticles (see text). The minimum between the peaks in the inset spectrum could be due to the presence of dark states or the absence of any state(s). See Figure 3 for distinction.

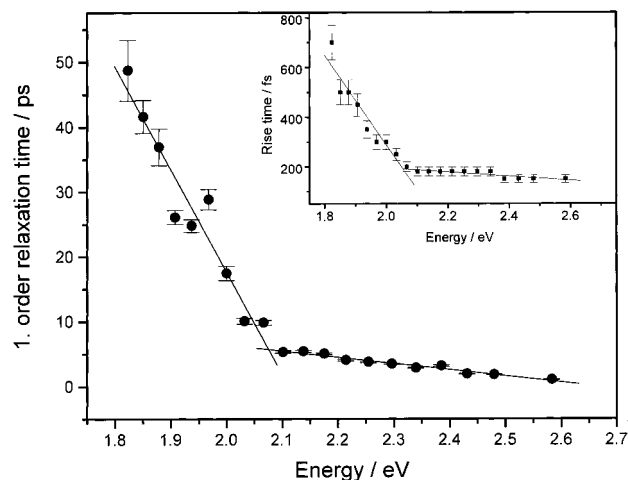


Figure 3. First-order decay times and rise times (inset) of the optical hole as monitored in the two different wavelength regions corresponding to the two peaks seen in the inset of Figure 2. Pumping is carried out at 400 nm. The fact that the decay times of the bleach in the high-energy region differ greatly from the rise times in the low-energy region suggest the presence of intervening dark states. They are blamed for the slow relaxation observed in the QDQW particles. The solid lines represent linear regressions on the experimental data points. The two lines intersect at 2.08 eV in excellent agreement with the observed minimum in the second-derivative spectrum and the energy calculated for the dark states,¹ one of which is the charge-separated state (see discussion).

examined in the 2.1–2.6 eV (the high-energy optically allowed) region and in 1.8–2.1 eV (the low-energy allowed) region. The high-energy bleach forms and decays much faster than the low-energy one. These wavelength regions fall within the two different bands in the derivative spectrum of the broad bleach spectrum shown in the inset of Figure 2. Furthermore, the decay times of the high-energy region do not correspond to the formation times of the low-energy region. This suggests the presence of dark state(s) between the two optically observed states and a nonconsecutive kinetic scheme for the relaxation dynamics in which the dark state is populated from the initially

excited state. The energy at which the rise and decay times change is determined to be at 2.08 eV. This is also the minimum of the inset spectrum. One can thus determine that the energy of the dark state(s) is 2.10 ± 0.05 eV.

For the size of the QWQD used in the present study, we were able to determine the predicted energies of the dark states by using Figure 3A in ref 1. For the size of our particles, two dark states, the $(2S_{3/2} - 1S)$ and $(1S_{1/2} - 1S)$ are calculated to be at energies of 2.10 and 2.16 eV, respectively. In the $1S_{1/2} - 1S$ state, the hole is in the CdS clad and the electron is in the HgS well. It is difficult to assign the experimentally determined level(s) to either of the calculated ones. It is also difficult to determine whether the observed slow dynamics is a result of the interconversion between these two levels or the relaxation between one of them and the optically allowed levels. Theoretical calculations of the rate of the different nonradiative processes need to be carried out to assist in determining the detailed relaxation mechanism. However, it was pointed out by Jaskolski and Bryant¹ that the $1S_{1/2}$ hole state does not get trapped in the HgS well because the hole has a very different effective mass in the CdS than in the HgS shell. As a result, the HgS shell acts as a barrier for the $1S_{1/2}$ hole rather than a well.¹ It is because of this that we propose that the observed dependence of the rate of the nonradiative relaxation process and its slow dynamics compared to the QD system are manifestations of the barrier effect in heterostructural nanoparticles in which the materials used have such a large difference in their band gap energies (0.50 eV for HgS and 2.5 eV for CdS) and the charged particles have different effective masses. Thus, in these types of heterostructures, charge separation does not only give rise to optically dark states but also to nonradiatively, slowly decaying, high-energy excitonic states.

Acknowledgment. The authors thank Dr. Garrett W. Bryant of NIST for sending us prior to publication his paper on "Multiband Theory of Quantum-Dot Quantum-Well: Dark Excitons, Bright Excitons and Charge Separation in Hetero-nanostructures" (ref 1). We thank the Office of Naval Research (through Grant No. N00014-95-1-0306). S.L. and R.B.L. thank the Georgia Tech Molecular Design Institute (Contract No. N00014-95-1-1116 from the Office of Naval Research) for partial financial support. S.L. thanks the German FCI and BMBF, and C.B. thanks the DAAD for a postdoctoral fellowship.

References and Notes

- (1) Jaskolski, W.; Bryant, G. W. *Phys. Rev. B* **1998**, 57, 4237.
- (2) O'Neil, M.; Marohn, J.; McLendon, G. M. *J. Phys. Chem.* **1990**, 94, 4356.
- (3) Misawa, K.; Yao, H.; Hayashi, T.; Kobayashi, T. *Chem. Phys. Lett.* **1991**, 183, 113.
- (4) Hasselbarth, A.; Eychmuller, A.; Weller, H. *Chem. Phys. Lett.* **1993**, 203, 271.
- (5) Wang, Y.; Suna, A.; McHugh, M.; Hilinski, E. F.; Lucas, P. A.; Johnson, R. D. *J. Chem. Phys.* **1990**, 92, 6927.
- (6) Zhang, J. Z.; O'Neil, R. H.; Roberti, T. W.; McGowen, J. L.; Evans, J. E. *Chem. Phys. Lett.* **1994**, 218, 479.
- (7) Kamat, P. V.; Dimitrijevic, N. M.; Fessenden, R. W. *J. Phys. Chem.* **1987**, 91, 386.
- (8) Kamat, P. V.; Ebbesen, T. W.; Dimitrijevic, N. M. *Chem. Phys. Lett.* **1989**, 157, 384.
- (9) Haase, M.; Weller, H.; Henglein, A. *J. Phys. Chem.* **1988**, 92, 4706.
- (10) Henglein, A. *Chem. Rev.* **1989**, 89, 1861.
- (11) Rossetti, R.; Hull, R.; Gibson, J. M.; Brus, L. E. *J. Phys. Chem.* **1985**, 82, 552.
- (12) Chestnoy, N.; Harris, T. D.; Hull, R.; Brus, L. E. *J. Phys. Chem.* **1986**, 90, 3393.
- (13) Eychmuller, A.; Hasselbarth, A.; Katsikas, L.; Weller, H. *Ber. Bunsen-Ges. Phys. Chem.* **1991**, 95, 79.
- (14) Serpone, N.; Sharma, D. K.; Jamieson, M. A.; Graetzel, M.; Ramsen, J. J. *Chem. Phys. Lett.* **1985**, 115, 473.
- (15) Barzykin, A. V.; Fox, M. A. *Isr. J. Chem.* **1993**, 33, 21.
- (16) Klimov, V.; Haring-Bolivar, P.; Kurz, H. *Phys. Rev. B* **1996**, 53, 1463.
- (17) Klimov, V. I.; Haring-Bolivar, P.; Kurz, H.; Karavinski, V. A. *Superlattices Microstruct.* **1996**, 20, 395.
- (18) Klimov, V.; Hunch, S.; Kurz, H. *Phys. Status Solidi B* **1995**, 188, 259.
- (19) Bawendi, M. G.; Wilson, W. L.; Rotherg, L.; Carrol, P. J.; Jedju, T. M.; Steigerwald, M. L.; Brus, L. E. *Phys. Rev. Lett.* **1990**, 65, 1623.
- (20) Nuss, M. C.; Zinth, W.; Kaiser, W. *Appl. Phys. Lett.* **1986**, 42, 1717.
- (21) Schoenlein, R. W.; Mittleman, D. M.; Shiang, J. J.; Alivisatos, A. P.; Shank, C. V. *Phys. Rev. Lett.* **1993**, 70, 1014.
- (22) Kharchenko, A.; Rosen, M. J. *Lumin.* **1996**, 70, 158.
- (23) Bawendi, M. G.; Carroll, P. J.; Wilson, W. L.; Brus, L. E. *J. Chem. Phys.* **1992**, 96, 946.
- (24) Mews, A.; Eychmuller, A.; Giersig, M.; Schooss, D.; Weller, H. *J. Phys. Chem.* **1994**, 98, 934.
- (25) Mews, A.; Kadavanich, A. V.; Banin, U.; Alivisatos, A. P. *Phys. Rev. B* **1996**, 53, 13242.
- (26) Bryant, G. *Phys. Rev. B* **1995**, 53, 16997.
- (27) Kamalov, V.; Little, R.; Logunov, S.; El-Sayed, M. A. *J. Phys. Chem.* **1996**, 100, 6381.
- (28) Logunov, S.; Green, T. C.; Marguet, S.; El-Sayed, M. A. *J. Phys. Chem.*, in press.